nature structural & molecular biology

Rapid spontaneous accessibility of nucleosomal DNA

Gu Li[1], Marcia Levitus[2,5], Carlos Bustamante[2–5] & Jonathan Widom[1]

DNA wrapped in nucleosomes is sterically occluded, creating obstacles for proteins that must bind it. How proteins gain access to DNA buried inside nucleosomes is not known. Here we report measurements of the rates of spontaneous nucleosome conformational changes in which a stretch of DNA transiently unwraps off the histone surface, starting from one end of the nucleosome, and then rewraps. The rates are rapid. Nucleosomal DNA remains fully wrapped for only ~250 ms before spontaneously unwrapping; unwrapped DNA rewraps within ~10–50 ms. Spontaneous unwrapping of nucleosomal DNA allows any protein rapid access even to buried stretches of the DNA. Our results explain how remodeling factors can be recruited to particular nucleosomes on a biologically relevant timescale, and they imply that the major impediment to entry of RNA polymerase into a nucleosome is rewrapping of nucleosomal DNA, not unwrapping.

Eukaryotic genomic DNA is organized in a repeating array of nucleosomes, in which short stretches of DNA, 147 base pairs (bp) in length, are wrapped locally in ~1 3/4 superhelical turns around octameric spools of histone proteins[1,2]. This nucleosomal organization of DNA makes most of the eukaryotic genome inaccessible to the many proteins that must bind to it for gene regulation, transcription, replication, recombination and repair. How such proteins gain needed access to nucleosomal DNA is not known[3–5].

Access to buried stretches of nucleosomal DNA may sometimes require the action of ATP-dependent nucleosome remodeling factors, which unwrap nucleosomal DNA, or drive nucleosomes to new locations along DNA[4,6–8]. An unanswered question is how such remodeling factors know which nucleosomes to remodel. A growing body of evidence suggests that remodeling factors are recruited to specific nucleosomes by site-specific DNA-binding proteins[9,10], raising in a chicken and egg–like fashion the question of how those DNA-binding proteins gain access to their own target sites.

Remodeling factors may not always be required to allow access to nucleosomal DNA. Nucleosomes spontaneously undergo conformational fluctuations (termed 'site exposure'), in which a stretch of their DNA transiently lifts off the histone surface, allowing free (but transient) access to proteins that would not otherwise be able to bind. The equilibrium constants describing this DNA accessibility are as large as ~10^{-2}–10^{-1} for sites located a short distance inside the nucleosome, decreasing to ~10^{-4}–10^{-5} for sites located near the middle of the nucleosome[11,12]. Studies using fluorescence resonance energy transfer (FRET)[13] reveal that site exposure involves large increases in separation between a fluorescence donor on one end of the nucleosomal DNA and a fluorescence acceptor on the histone core, implying that site exposure occurs by progressive unwrapping of the nucleosomal DNA starting from one end of the nucleosome[14] (**Fig. 1**).

A consequence of this inherent behavior of nucleosomes, confirmed in the FRET analysis, is that when nucleosomal DNA contains a target sequence for a sequence-specific DNA-binding protein, the mere presence of that protein in solution causes nucleosomes to respond by shifting their conformational equilibrium toward the exposed, unwrapped state, simultaneously allowing stable binding by the protein. Site exposure occurs spontaneously; the conformational equilibrium shifts in accord with principles of physical chemistry.

Although previous studies revealed and quantified equilibrium aspects of this underlying behavior of nucleosomes, no measurements have been made of the actual rates of spontaneous DNA unwrapping or rewrapping. The rates of site exposure and rewrapping (k_{12} and k_{21}, respectively, **Fig. 1**) are of interest because they provide insight into the molecular mechanisms of remodeling factor action, and on other fundamental questions in gene regulation. Knowledge of the rate of site exposure will help distinguish whether remodeling factors act simply as brownian ratchets, trapping and harnessing spontaneous nucleosome unwrapping events as they occur[15], or whether they actively drive DNA off the nucleosome[16,17]. The rate of spontaneous site exposure also sets an upper limit on the rate at which regulatory proteins can occupy a specific target site by passive binding. Conversely, the rate of spontaneous rewrapping defines a benchmark for kinetic efficiency in regulation by passive binding proteins: an efficient system requires that the rate at which a protein encounters a transiently exposed binding site *in vivo* be comparable to or greater than the rate at which the transiently exposed site is spontaneously rewrapped, k_{21}.

In an earlier study, we used a bacteriophage RNA polymerase as a reporter of accessibility of nucleosomal DNA, and found that access by the polymerase to sites along the full length of the nucleosome can occur in several seconds or less. If one assumes that the polymerase can move forward only after DNA has already unwrapped, then the observed rate

[1]Department of Biochemistry, Molecular Biology, and Cell Biology, Northwestern University, Evanston, Illinois 60208-3500, USA. [2]Department of Physics, [3]Department of Molecular and Cell Biology, [4]Biophysics Graduate Group and [5]Howard Hughes Medical Institute, University of California, Berkeley, California 94720, USA. Correspondence should be addressed to J.W. (j-widom@northwestern.edu).

Published online 5 December 2004; doi:10.1038/nsmb869

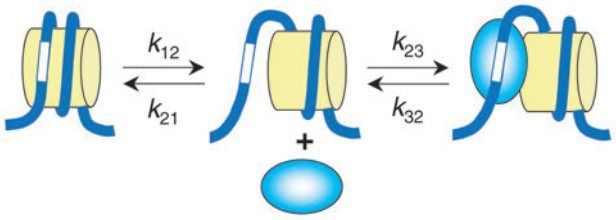

Figure 1 Mechanism of site exposure in nucleosomes deduced from earlier studies[11,14]. Fully wrapped nucleosomes (left) are in dynamic equilibrium with transient states (middle) in which a stretch of DNA has unwrapped off the histone core, starting from one end of the nucleosome. During moments when the DNA is unwrapped, site-specific DNA-binding proteins (blue ellipse) gain passive access to otherwise-buried target sites and can bind to make a complex (right). The goal of the present study is to measure the rates of site exposure (k_{12}) and rewrapping (k_{21}).

of polymerase elongation would equate to a lower bound on the rate constant for DNA unwrapping of $k_{12} \geq 0.13\ s^{-1}$ (ref. 18). However, the actual rates of unwrapping and rewrapping were not measured in that study, and the assumption that the polymerase did not influence the unwrapping rate could not be tested.

The goal of the present study was to determine the actual rates of spontaneous unwrapping and rewrapping of nucleosomal DNA. We took two approaches, both using reagents developed in our earlier FRET study[14]. One approach uses stopped-flow FRET to measure the rate at which nucleosomes spontaneously unwrap to allow binding by a passive site-specific DNA-binding protein. A second approach is based on fluorescence correlation spectroscopy (FCS) of small numbers of nucleosomes at a time, diffusing freely in dilute solution[19–21]. The results from the two approaches are in good agreement. The rate of spontaneous nucleosome unwrapping is ~4 s^{-1}, fast enough such that passive binding by regulatory proteins to spontaneously exposed nucleosomal target sites can occur quickly relative to other events in gene expression. The rate of rewrapping is ~20–90 s^{-1}, setting tight limits for kinetic efficiency in regulation and leading to the conclusion that the major impediment to RNA polymerase translocation into a nucleosome is rewrapping of nucleosomal DNA, not unwrapping.

RESULTS

Stopped-flow FRET system

In the stopped-flow experiments, our strategy was to measure the rate at which nucleosomes spontaneously unwrap to allow stable binding by an arbitrary site-specific DNA-binding protein, in our case, the LexA repressor protein of *Escherichia coli*. Nucleosome unwrapping is detected by changes in FRET between a fluorescence donor placed at a DNA end, near the binding site for LexA protein, and a fluorescence acceptor attached to the histone core. Spontaneous unwrapping of the nucleosome, stabilized by rapid LexA binding, increases the distance between the two FRET dyes, thereby decreasing the FRET efficiency. At a sufficiently high LexA concentration ([LexA]), the observed rate is limited by the inherent spontaneous unwrapping rate of the nucleosome itself, thus yielding a measurement of k_{12}. k_{21} is then calculated from k_{12} together with the previously measured site exposure equilibrium constant, $K_{eq} = k_{12} / k_{21}$. We chose LexA protein for these studies because it is frequently used in fusion proteins to bring other gene regulatory protein domains to specific locations in chromatin in diverse eukaryotic organisms and cell types, and its equilibrium binding to nucleosomal target sites is well understood[11,14].

Nucleosomes were prepared centered on a 147-bp nucleosome positioning DNA (**Fig. 2a**). A target site for LexA was introduced a short distance inside from one end of the nucleosomal DNA, nearby the fluorescence donor dye (D, Cy3), which was attached at a DNA 5′ end. The fluorescence acceptor dye (A, Cy5), was attached using maleimide chemistry to a unique sulfhydryl on histone H3 V35C C110A, located on the histone core nearby the 5′ end of the wrapped DNA. The histone octamer of the nucleosome contains two copies each of the four core histones, hence each A-labeled nucleosome will contain two molecules of A. The FRET efficiency (E) depends strongly on the ratio of the actual D-A distance to a characteristic transfer distance (R_0), which, for the Cy3-Cy5 dye pair, is ~6 nm (ref. 22). The crystal structure of the nucleosome[2] implies that the real distance (R) from D to the two symmetry-related molecules of A is ~2 nm and ~8 nm, respectively. Because one of these distances is much less than R_0, we observe highly efficient FRET for nucleosomes in their predominant conformation at physiological or lower ionic strength (**Fig. 2b**). The FRET efficiency is 100%; we observe residual D emission because the labeling by A is incomplete, only ~80% (ref. 14).

As expected, titration of these nucleosomes with increasing [LexA] is accompanied by a progressive and saturable decrease in FRET, as can be seen from an increase in emission from D and decrease in emission from A (**Fig. 2b**). The titration saturates at a value of FRET efficiency ~0.4, implying that, in the fully occupied nucleosomes, the distance from D to the nearer A increased greatly, to ~6.4 nm (ref. 14).

We measured the rate of this FRET change by rapidly adding a high concentration of LexA such that site exposure itself is rate limiting, and the observed rate equals k_{12} (see Methods). The high [LexA] regime is

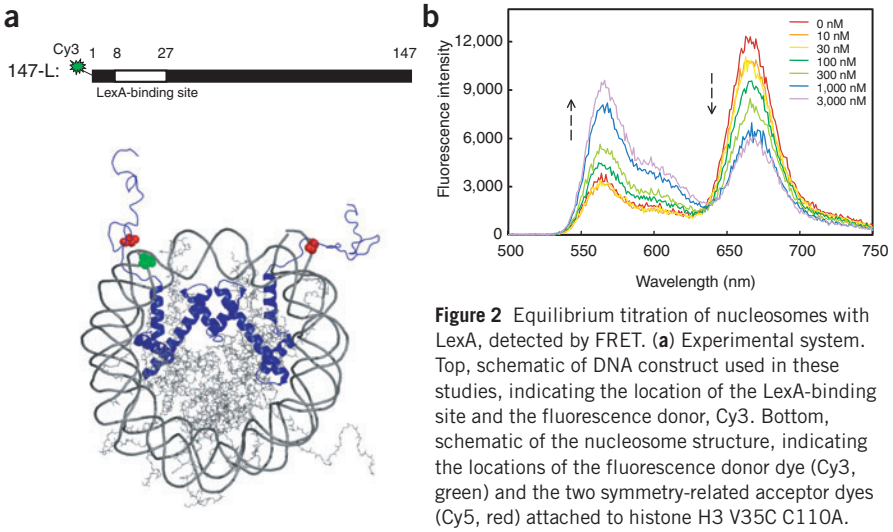

Figure 2 Equilibrium titration of nucleosomes with LexA, detected by FRET. (**a**) Experimental system. Top, schematic of DNA construct used in these studies, indicating the location of the LexA-binding site and the fluorescence donor, Cy3. Bottom, schematic of the nucleosome structure, indicating the locations of the fluorescence donor dye (Cy3, green) and the two symmetry-related acceptor dyes (Cy5, red) attached to histone H3 V35C C110A. Histone H3 is blue; the other histones are gray, dimmed for clarity. This system exhibits ~100% FRET efficiency. Residual D emission results from incomplete chemical labeling by A. (**b**) LexA titration. Emission spectra from doubly labeled (D-A) nucleosomes, titrated with increasing concentrations of LexA. Increasing LexA leads to increased D emission and decreased A emission (arrows), implying that nucleosomes spend a greater fraction of time partially unwrapped, coupled to the binding of LexA. The FRET efficiency, E, decreases from ~100% in the absence of LexA to ~40% at near-saturating [LexA] corresponding to a change in D-A separation distance from ~2 nm (fully wrapped with high probability, at 0 LexA) to ~6.4 nm (substantially unwrapped with high probability, at the highest [LexA]).

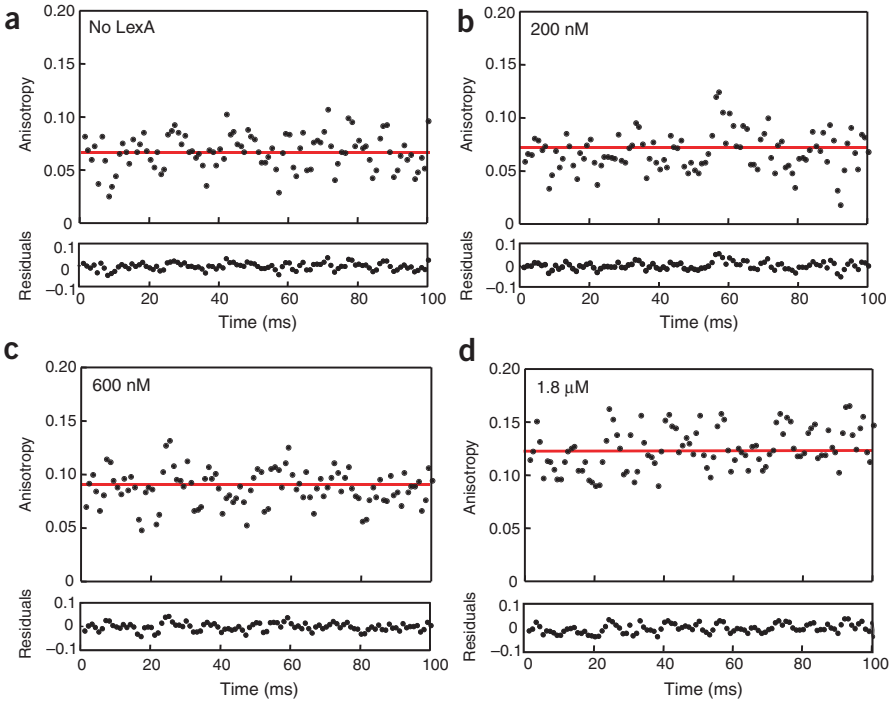

Figure 3 Kinetics of LexA binding to DNA monitored by stopped-flow fluorescence anisotropy. The first 100 ms are shown; horizontal lines show averages of the data. Top graphs, measured data; bottom graphs, residual differences from the measured average. (**a**) No LexA. Fluorescein emission anisotropy was constant at ~0.062. (**b**) LexA (200 nM). Anisotropy was constant at ~0.069. The change in anisotropy is too small to state with confidence the time required for the anisotropy to reach this equilibrium value. (**c**) LexA (600 nM). Anisotropy was constant at ~0.082. Binding was complete within 2 ms, implying that k_{23} must be $> 5 \times 10^8$ M^{-1} s^{-1}, as expected for protein-DNA interactions. (**d**) LexA (1.8 μM). Anisotropy was constant at ~0.13.

defined by the requirement that $k_{23} \times [\text{LexA}] >> k_{21}$. The rate constant for binding of proteins to specific DNA target sites is often extremely fast, comparable to or faster than the diffusion-controlled limit of ~10^9 M^{-1} s^{-1} (refs. 23,24); thus, even modest [LexA] will prove sufficient to reach the desired kinetic regime. To be certain that our experiment was properly in the high [LexA] regime, we confirm below that the observed rate is independent of [LexA], and that $k_{23} \times [\text{LexA}] > k_{21}$. This latter test required that we measure k_{23}.

LexA-DNA association rate

We used stopped-flow fluorescence anisotropy to place a lower bound on k_{23} (**Fig. 3**). DNA of 32 bp in length was used to approximate the situation in which a stretch of DNA a little longer than the LexA target site has unwrapped to allow LexA binding in a nucleosome. The DNA was labeled with fluorescein at one 5′ end and ^{32}P at the other, allowing measurement of equilibrium LexA binding either by native gel electrophoresis or fluorescence anisotropy, and allowing measurement of the kinetics of binding from changes in anisotropy over time. Binding occurred instantaneously on the stopped-flow time scale (completion within 2 ms) (**Fig. 3**), implying that $k_{23} > 5 \times 10^8$ M^{-1} s^{-1}, as expected for protein-DNA interactions. The anisotropies measured by stopped flow throughout the entire time course equaled the values measured in equilibrium titrations (**Fig. 4**), confirming that the full binding process was observed in the kinetic experiments.

Stopped-flow FRET results

We next used stopped-flow FRET, monitoring the kinetics of nucleosome unwrapping after rapid addition of LexA, to determine k_{12}. With 200 nM LexA (**Fig. 5**), binding occurred quickly, as a single-exponential relaxation process, with an apparent rate constant $k_{app} = 3.9 \pm 0.9$ s^{-1} ($n = 3$). A 15-fold increase in [LexA] did not result in any changes to this observed fast rate (**Supplementary Fig. 1** and **Supplementary Table 1** online), implying that even the 200 nM LexA measurements are already in the high [LexA] regime. Thus, $k_{12} \cong k_{app} = 3.9 \pm 0.9$ s^{-1}. The

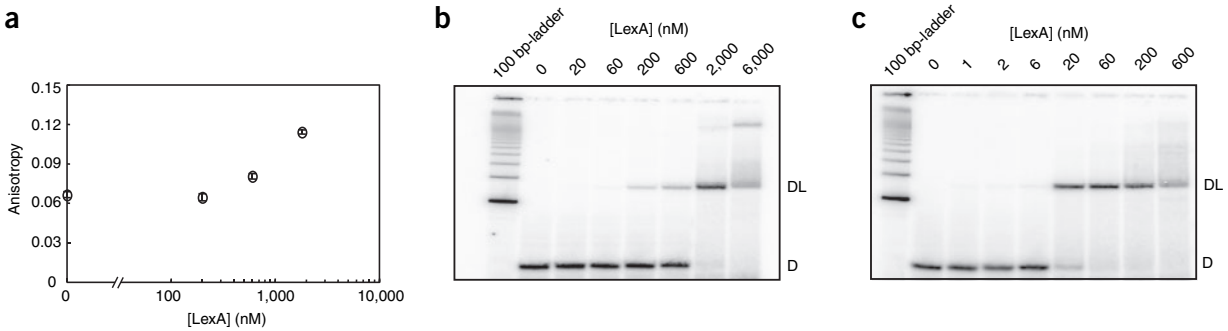

Figure 4 Equilibrium binding of LexA to DNA. (**a**) LexA binding measured by fluorescence anisotropy. DNA F-32 (200 nM) was titrated with 0, 200 nM, 600 nM or 1.8 μM LexA. Data points and error bars, means and s.d. ($n = 3$). The measured anisotropies increased with [LexA] from ~0.063 to ~0.12. (**b**) LexA binding to DNA monitored by native gel electrophoresis in the same conditions as in **a**. DNA F-32 (200 nM) was titrated with increasing [LexA] (indicated). D, free DNA F-32; DL, DNA–LexA complexes. LexA bound with a transition midpoint (EC_{50}) of ~600–2,000 nM. The results confirm that the anisotropy increases in **a** properly reflect the binding process. (**c**) LexA binding to DNA at low [DNA], for comparison with earlier studies[14]. DNA F-32 (1 nM) was titrated with purified LexA protein (indicated). LexA bound with a transition midpoint (EC_{50}) of ~6–20 nM. As expected (see Methods), at 200 nM DNA the equilibrium LexA-binding curve (measured either by fluorescence anisotropy or native gel electrophoresis) shifted to higher [LexA] than is required for binding at the low DNA or nucleosome concentrations used in the more sensitive FRET studies (compare **Figs. 4a** and **2b**, and **Figs. 4b** and **4c**). This does not alter our conclusion that $k_{23} > 5 \times 10^8$ M^{-1} s^{-1}.

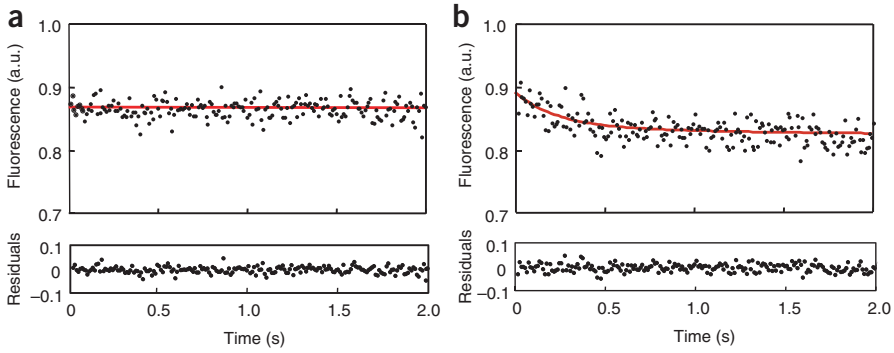

Figure 5 Stopped-flow FRET analysis of LexA binding to nucleosomes. The time range 0–2 s was sampled with 200 equally spaced points. (**a**) Mock reaction with no LexA. Cy5 fluorescence emission intensity (arbitrary units) measured as a function of time. No time-dependent decrease of FRET was detected. Top graph, measured data and least-squares fit to a constant; bottom graph, residuals. (**b**) Reaction with [LexA] = 200 nM (after mixing), a concentration sufficiently high such that the observed rate is limited by the rate of spontaneous nucleosome opening (see text). Top graph, measured data and least-squares fit to a single exponential; bottom graph, residuals. Fits to two exponentials yielded two identical rate constants (results not shown), implying that the data are dominated by a single-exponential process. The zero-time intercept of the fit curve equals that for the mock reaction (**a**), ruling out the possibility that a hypothetical additional process contributing a substantial FRET change could have occurred on too rapid a timescale to detect.

observed FRET signal decays from an initial value that is equal to that from a mock reaction with no LexA (**Fig. 5a**), thus, no additional faster process leading to substantial FRET change could have been missed in these experiments.

Our earlier FRET study yielded several estimates of the equilibrium constant for site exposure, K_{eq} (ref. 14). The observed reduction of LexA binding affinity for binding to nucleosomes versus naked DNA (in the same solution conditions as used here) implies that $K_{eq} \cong 0.02$–0.03, whereas the FRET intensities themselves imply $K_{eq} \cong 0.02$–0.1 (over a wide range of subphysiological ionic strengths). The geometric average of these measurements yields $K_{eq} \cong 4.5 \times 10^{-2}$, from which we calculate $k_{21} = k_{12} / K_{eq} \cong 90\ s^{-1}$.

Given that $k_{23} > 5 \times 10^8\ M^{-1}\ s^{-1}$ (**Fig. 3**), $k_{21} \cong 90\ s^{-1}$ satisfies the condition $k_{23} \times [LexA] > k_{21}$ even for the lowest [LexA] investigated, 200 nM. Thus, our analysis is self-consistent in its conclusion that all of the measurements are in the desired high [LexA] (opening-limited) kinetic regime.

FCS analysis

To check the conclusions of this kinetic analysis, we used an unrelated approach, FCS, to directly monitor spontaneous unwrapping and rewrapping events in small numbers of nucleosomes at a time, in free solution. Our strategy was to compare fluctuations of fluorescence donor emission intensity for samples labeled with donor only, with the fluctuations from samples labeled with a FRET D-A dye pair. Donor intensity fluctuations are quantified by their autocorrelation function, which reflects any process that gives rise to fluctuations in the fluorescence signal[20,21]. For nucleosomes labeled with D alone, only diffusion of the nucleosomes into and out of the confocal volume is expected to produce donor intensity fluctuations; however, for D-A double-labeled nucleosomes, both diffusion and intramolecular conformational dynamics that change the FRET efficiency (such as transient DNA unwrapping) result in donor intensity fluctuations. The ratio of the fluorescence donor autocorrelation functions obtained from nucleosomes labeled with FRET donor only, or with both donor and acceptor, yields two equations relating the two unknown rates, k_{12} and k_{21}, allowing each to be determined individually[19–21].

Nucleosomes were prepared labeled with D only[14] or with the D-A pair (**Fig. 2**). Fluorescence donor emission autocorrelation functions were obtained for dilute solutions of each sample (**Fig. 6a**). As expected, the autocorrelation function for D-only nucleosomes fit well to a model based on diffusion only (results not shown). Compared with the autocorrelation function for D-only nucleosomes, the autocorrelation function for D-A nucleosomes reveals no additional relaxation processes over the microsecond-to-millisecond timescale. This means that D-A nucleosomes have no dynamics resulting in substantial FRET changes over these timescales. This confirms a conclusion from our stopped-flow studies, namely that all LexA-dependent changes in FRET efficiency that occur were detected in those experiments and that they occur only on a longer timescale (hundreds of milliseconds).

The ratio of the normalized fluctuation autocorrelation functions recorded for D-A nucleosomes and D-only nucleosomes ($G_{DA}(\tau)$ / $G_D(\tau)$; **Fig. 6b**), isolates contributions due to chemical kinetics from those due to diffusion, and yields the sum and ratio of the kinetic rate constants k_{12} and k_{21} (see Methods). Fitting the data in **Figure 6b** to the diffusion-reaction mechanism (equation (10)) yields $k_{12} / k_{21} = 0.18$ and $k_{12} + k_{21} = 23.6\ s^{-1}$, from which we calculate $k_{21} = 20\ s^{-1}$ and $k_{12} = 3.6\ s^{-1}$.

The ratio k_{12} / k_{21} is obtained from the amplitude of the observed exponential relaxation in $G_{DA}(\tau)$ / $G_D(\tau)$ (see Methods), and thus is particularly sensitive to experimental variables such as sample concentrations, stability of the confocal volume, accuracy of the assumption $E_{FRET} = 1$ (when fully wrapped), among others. However, the term $(k_{12} + k_{21})$, which is determined from the rate of the observed relaxation, is independent of or only slightly dependent on these factors, and is thus more reliably determined. Because $k_{21} >> k_{12}$ ($K_{eq} << 1$), the calculated relaxation rate is approximately equal to the fastest process, which is the rewrapping rate. Thus, we expect that these experiments yield the rewrapping rate with more accuracy than the unwrapping rate. In fact, the results for both the unwrapping and rewrapping rates are in good agreement with those obtained using the stopped-flow mixing method. We conclude that, for nucleosomes in these solution conditions, $k_{12} \cong 4\ s^{-1}$, and $k_{21} \cong 20$–$90\ s^{-1}$.

DISCUSSION

Rapid spontaneous site exposure in nucleosomes

Two very different experiments—one monitoring the rate of unwrapping of nucleosomal DNA, trapped by protein binding, in bulk solution, the other monitoring the rates of unwrapping and rewrapping, in the absence of a binding protein, in a small number of nucleosomes at a time—both point to the same conclusion: nucleosomal DNA spontaneously unwraps and rewraps, on timescales fast compared with seconds. Both experiments lead to estimates for the unwrapping rate constant (k_{12}) of ~4 s^{-1}, and to estimates for the rewrapping rate constant (k_{21}) of ~20 to ~90 s^{-1} (from FCS and stopped flow, respectively). The differences in the rates measured from the two experiments are insignificant at this level of analysis; they are comparable to the uncertainty in the previously measured value of K_{eq} itself, and could reflect experimental error or a breakdown of the two-state assumption that is inherent in both analyses. We conclude that spontaneous

unwrapping and rewrapping of nucleosomal DNA occur rapidly.

Earlier studies show that the ability of Gal4 protein[25,26] and the restriction enzyme SalI[27] to access target sites inside a nucleosome is not an 'end effect,' unique to isolated nucleosomes, but instead is similar (Gal4) or quantitatively equivalent (SalI) for isolated nucleosomes and for a test nucleosome centered in an 11-mer polynucleosome. Therefore, we anticipate that the dynamic behavior of nucleosomes in long chains will resemble that studied here in single nucleosomes. Even the detailed rates may not change much, as the hydrodynamic drag exerted by neighboring nucleosomes is likely to chiefly affect processes on a microsecond-or-faster timescale[28]. Of course, if higher-order levels of chromatin structure prove to involve substantial nucleosome-nucleosome interactions (such as those stabilized by histone H1), this could affect nucleosome dynamics[29]. However, the role of H1 itself is not clear[30]. Although many earlier studies suggested a structural role for H1 (ref. 31), yeast are viable without it[32]. The available data suggest instead that, at least in yeast, H1 has a subtle regulatory role[33,34], and that some or all major biological functions of chromatin do not depend on it. For these reasons, many groups appropriately use polynucleosomes lacking H1 as model systems with which to analyze chromatin structure and function *in vitro*.

Both experiments agree that no additional faster nucleosome opening processes contributing substantial FRET changes could have existed but been missed. We note, however, that because the distance from D to A in the wrapped DNA is ~2 nm whereas R_0 is ~6 nm, motions of the DNA ends over distances of less than ≤2 nm would be expected to produce only negligible changes in FRET and so would not be detectable in either experiment.

The opening rate constant (k_{12}) of ~4 s^{-1} corresponds to a lifetime in the fully wrapped state ($\tau_{wrapped}$) = 1 / k_{12} ≅ 250 ms. Nucleosomes in solution look like those imaged by crystallography only for very short periods of time, <<1 s, before undergoing a large-scale spontaneous unwrapping event. The rewrapping rate constant (k_{21}) of ~20–90 s^{-1} corresponds to a lifetime in the unwrapped state ($\tau_{unwrapped}$) = 1 / k_{21} ≅ 10–50 ms. Once unwrapped, nucleosomes wait only a very short time before rewrapping their DNA.

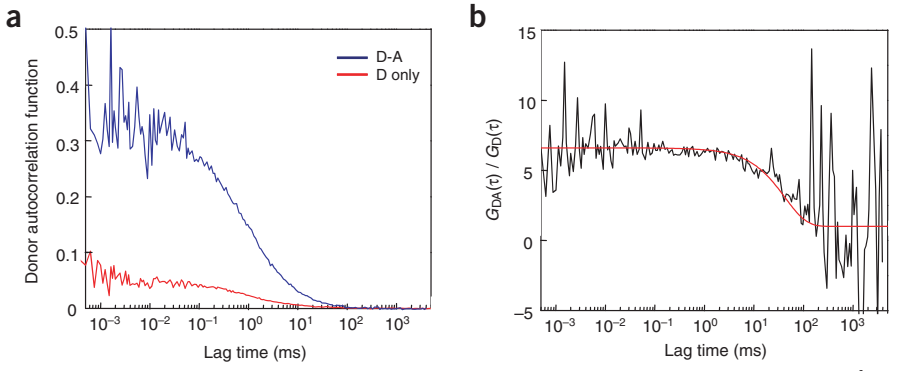

Figure 6 Spontaneous nucleosome opening and rewrapping fluctuations detected by fluorescence correlation spectroscopy. (**a**) Cy3 emission autocorrelation functions for nucleosomes labeled with D only or with both D and A, at identical concentrations. The autocorrelation function for the D-only nucleosomes fits well to a model based on diffusion only (results not shown). (**b**) Ratio of curves in **a**. The ratio isolates contributions to the Cy3 autocorrelation function due to FRET fluctuations in the D-A double-labeled nucleosomes from contributions due to diffusion. Solid line, least-squares fit to equation (10), providing two equations for the two unknown rate constants, k_{12} and k_{21}.

Implications for gene regulation

These rates and lifetimes place constraints on mechanisms of gene regulation, nucleosome remodeling, transcription and replication. There are two important constraints with regard to gene regulation. Nucleosome opening needs to be fast enough so as not to impede the regulatability of genes on required timescales. A wrapped state lifetime of ~250 ms means that accessibility at a given locus would essentially never be delayed because of nucleosome structure by more than a second or so. Such times are short compared with documented timescales for gene regulation *in vivo* and, especially, for gene transcription (see below) and protein synthesis. We conclude that the spontaneous opening rate of nucleosomes suffices to account for what is known at present about the regulatability of genes.

A second constraint is that for regulation to be kinetically efficient, a transiently exposed target site needs to be recognized and bound by a regulatory protein within the (brief) open state lifetime, which we show is only ~10–50 ms. At present, no information is available about the actual rates of regulatory protein binding *in vivo*. DNA looping may greatly accelerate rates of regulatory protein binding *in vivo* by enhancing the effective local concentrations[35].

Implications for nucleosome remodeling

Nucleosome remodeling factors could act as brownian ratchets by trapping and harnessing spontaneous nucleosome unwrapping events as they occur[15]. In this case, the overall rate of nucleosome remodeling would be limited by the rate of spontaneous nucleosome unwrapping, ~4 s^{-1}. Alternatively, remodeling factors could actively drive DNA off the nucleosome surface, accelerating the rate of DNA release[16,17]. It will be interesting to test whether remodeling factors enhance the microscopic rate constant for nucleosome opening. Existing *in vitro* studies indicate that the remodeling factor SWI/SNF remodels nucleosomes with a k_{cat} for ATP hydrolysis of ~1–2 s^{-1} (ref. 36) or ~10 s^{-1} (ref. 17), but it remains unclear how much DNA is unwrapped per ATP hydrolyzed, so a direct comparison of those results with our measurement of k_{12} is not yet possible.

Implications for nucleosome transcription

Finally, our results lead to the conclusion that nucleosome rewrapping, not unwrapping, is the chief obstacle hindering the entry of RNA polymerase II (Pol II) into a nucleosome. Pol II elongates at a rate of only ~23 nucleotides s^{-1} (ref. 37) (that is, ~2 s for a typical ~40–50-bp linker between nucleosomes, and another ~6–7 s for the nucleosomal DNA itself), whereas nucleosome unwrapping occurs spontaneously much more rapidly, on average within just ~250 ms. Thus, a Pol II molecule, engaged on linker DNA and approaching the next fully wrapped nucleosome, would be negligibly delayed by a requirement for nucleosome unwrapping to precede further polymerase progression. In contrast, spontaneous nucleosome rewrapping is an important hindrance. Once unwrapped, the nucleosome waits, on average, only ~10–50 ms before rewrapping. During such a short period, Pol II will often fail to progress by even one base pair. This means that the unwrapped DNA will often fully rewrap before the polymerase takes a step to advance into the nucleosome. Such unwrapping and rapid rewrapping events may recur many times before the polymerase successfully advances into the nucleosome. Accessory factors of the polymerase could facilitate its entry into a nucleosome simply by suppressing the rewrapping of transiently unwrapped nucleosomal DNA; such a mode of action would be far more

effective in enhancing the polymerase elongation rate than would active unwrapping of the nucleosomal DNA. Once inside the nucleosome, the sheer size of the polymerase should prevent further rewrapping of the DNA, and its elongation rate through the remainder of the nucleosome should be dominated by its intrinsic rate on naked DNA, and its ability to peel the DNA off the surface of the nucleosome as it transcribes.

METHODS

Preparation of DNA, proteins and nucleosomes. Individual nucleosomes were prepared centered on a 147-bp nucleosome positioning sequence, for which the single dominant position is known exactly[14]. The DNA was labeled at one 5′ end with the FRET donor dye, Cy3. A binding site for LexA protein was introduced near the labeled end, oriented such that the face of the DNA occupied by LexA pointed inward toward the histone core. The LexA site was located outside the region responsible for nucleosome positioning on this DNA[38].

DNA, histones and nucleosomes were prepared, purified and characterized as described[14]. Nucleosomes were prepared from recombinant *Xenopus laevis* histone octamer comprising H2A, H2B, H3 V35C C110A and H4. DNA (147 bp) was prepared by PCR and was labeled with Cy3 (FRET donor) by incorporation of an appropriate Cy3-labeled primer. The Cy3 dye was placed at the DNA 5′ end adjacent to the LexA-binding site. The PCR product was purified by reverse-phase HPLC. D-A double-labeled nucleosomes were prepared from histone octamer that had been labeled with Cy5 maleimide (FRET acceptor) at the unique cysteine on histone H3 V35C C110A. Nucleosomes were purified by sucrose gradient ultracentrifugation and checked for purity by native PAGE.

DNA construct F-32, which has a 5′ fluorescein (F) at one end and a 20-bp LexA-binding site in the middle, was prepared by annealing two oligos together: F-AACATGTAC-TGTATGAGCATACAGTAAGTCGA; and TCGACTTACTGTATGCTCATACAGTACA-TGTT (LexA-binding sequence is underlined).

LexA protein was purified from plasmid pJWL228 (gift of J. Little, University of Arizona, Tucson) as described[39].

Steady-state fluorescence spectra. A steady-state photon counting fluorometer (ISS, model PC1) was used for all steady-state fluorescence experiments. Fluorescence emission spectra were carried out as described[14], using 8 nM D or D-A nucleosomes in 0.5× TE (TE is 10 mM Tris, pH 7.5, 1 mM EDTA) with increasing concentrations of LexA. Excitation was done at 515 nm; emission spectra were collected from 500–750 nm with a 550-nm cut-on filter. Absolute FRET efficiency measurements were made as described[14] with direct excitation of Cy5 at 610 nm.

Stopped-flow kinetic measurements. Stopped-flow experiments were carried out using an Applied Photophysics model SX.18MV instrument at room temperature (~23 °C) in 0.5× TE buffer. Certain experiments included additional [NaCl] (see **Supplementary Data** and **Supplementary Figs. 1–3** online). LexA binding to nucleosomes was monitored by FRET, following the decrease in sensitized emission of Cy5. After rapid mixing, solutions contained 7 nM D-A-labeled nucleosomes, plus 0, 200 nM, 400 nM, 1 μM or 3 μM LexA protein. Excitation was done at 515 nm; a 645-nm cut-on filter was placed in the emission channel to isolate Cy5 emission. Data were collected for durations of 1, 2 or 10 s, sampled with 1,000 linearly spaced data points.

The kinetics of LexA binding to naked DNA was monitored by the increase in fluorescein emission anisotropy. Differing concentrations of LexA were rapidly mixed with a fluorescein-labeled 32-bp DNA containing a specific LexA target sequence. LexA binding was followed over time by the increase in fluorescence emission anisotropy. After rapid mixing, samples contained 200 nM F-32 DNA, plus 0, 200 nM, 600 nM or 1.8 μM LexA protein. Excitation was done with vertically polarized light at 485 nm. Two emission channels, both with 530-nm cut-on filters, were used to monitor the vertical and horizontal polarized emission components simultaneously. Fluorescence anisotropy data were collected for 1 s, sampled with 1,000 linearly spaced data points.

Equilibrium binding of LexA to DNA. The studies of **Figure 4** were carried out (i) to confirm that the stopped-flow measurements (**Fig. 3**) monitor the full LexA-binding process; and (ii) to relate LexA binding in the anisotropy experiments, which require relatively high [DNA] (200 nM) to LexA binding in the present FRET experiments, and in our earlier studies[14], which were carried out at much lower [DNA]. Because LexA binds to DNA as a monomer coupled to cooperative dimerization of bound monomers[40], the apparent affinity for LexA is greatly dependent on [DNA]: at high [DNA] (200 nM) and low [LexA] (for example, 10 nM), lower-affinity monomeric binding predominates, whereas at low [DNA] (1 or 7 nM), cooperative dimeric binding predominates even at low [LexA].

Steady-state fluorescence anisotropy measurements. Measurements were made using the ISS PC1, in the identical solution conditions used in the stopped-flow experiments. DNA F-32 (200 nM) in 0.5× TE was excited at 485 nm. The same 530-nm cut-on filter as used for the stopped-flow anisotropy measurements was placed in the emission channel.

Gel mobility shift assays. 147-L or F-32 DNA was labeled at 5′ ends with [γ-^{32}P]ATP using T4 polynucleotide kinase. DNA 147-L at 1 nM, or F-32 at 1 or 200 nM, was titrated with increasing concentrations of LexA protein at room temperature (~23 °C). Samples were incubated for 2 min at room temperature, and then loaded onto running 5% (w/v) nondenaturing polyacrylamide gels. Gels were dried and analyzed by phosphorimager.

Kinetic analysis. We represent the mechanism of **Figure 1** as

$$\mathrm{N} \underset{k_{21}}{\overset{k_{12}}{\rightleftharpoons}} \mathrm{S+R} \underset{k_{32}}{\overset{k_{23}}{\rightleftharpoons}} \mathrm{RS} \qquad (1)$$

where N is the fully wrapped nucleosome, S is the nucleosome after spontaneous site exposure, and R is an arbitrary regulatory protein, LexA repressor protein in our case. For such reversible two-step reactions, the relaxation kinetics are characterized by two relaxation times, one corresponding to flux from the two end states (N and RS) toward the intermediate (S + R), the other corresponding to flux from the intermediate toward the two ends[41]. For many such cases, the intermediate (S) is present at very low concentration and is in steady state. This is the expected situation for nucleosomes because (i) $K_{eq} = k_{12} / k_{21} << 1$, implying that $k_{21} >> k_{12}$; (ii) as will be seen, $k_{21} >> 1\ s^{-1}$, whereas ordinarily $k_{32} << 1\ s^{-1}$ for site-specific DNA-binding proteins; and (iii) we include experiments at very high [LexA], such that most of the nucleosomes are converted to RS, implying that $(k_{23} \times [R]) >> k_{32}$. Thus, $k_{21} + (k_{23} \times [R]) >> k_{12} + k_{32}$, from which it follows that [S] will always be negligible. Because of this, it is not possible to detect the relaxation corresponding to flux from S to (N and RS), and so we expect that only one relaxation time, corresponding to flux from two ends to the intermediate, will be observed. This one relaxation time will be manifested as a single-exponential decay in the observed FRET signal.

There are two important limits for equation (1) when S is in steady state[41]. Case I (low [LexA]) obtains when

$$k_{23} \times [\mathrm{LexA}] << k_{21} \qquad (2)$$

This is the rapid pre-equilibrium regime. In this situation, the single apparent relaxation rate, k_{app}, becomes

$$k_{app} = K_{eq} \times k_{23} \times [\mathrm{LexA}] \qquad (3)$$

Case II (high [LexA]) obtains when

$$k_{23} \times [\mathrm{LexA}] >> k_{21} \qquad (4)$$

This is the opening-limited regime. In this regime, the single apparent relaxation rate, k_{app}, becomes

$$k_{app} = k_{12} \qquad (5)$$

that is, the observed rate becomes independent of [LexA], and equals the rate of spontaneous nucleosome opening. This is the regime we use in the present study.

Fluorescence correlation spectroscopy. FCS measurements were carried out using a custom confocal optical system with a 1.3 NA × 100 microscope objective

(Zeiss Fluar) and a diode pumped 532-nm laser (Crystalaser) as the excitation source. The emitted fluorescence was collected using the same objective and passed through a pinhole of diameter 50 μm in the image plane of the objective. The fluorescence was then separated into the donor and acceptor components using a dichroic mirror, and the donor component was further divided in two using a 50:50 nonpolarizing beam splitter. Each component was filtered using a narrow bandpass filter (3rd Millennium series, Omega optical) and focused onto a photon-counting module (SPCM-AQR-14, Perkin Elmer Optoelectronics). The output of the Cy3 detectors was cross-correlated using a correlator (ALV-5000/EPP, ALV). This arrangement provides a way of removing after-pulsing artifacts in the Cy3 autocorrelation function. Instead of autocorrelating the signal in a single detector, the signal is split in two, detected by two independent detectors, and cross-correlated.

FCS was measured using a few microliters of a 100 nM solution of the fluorescently labeled nucleosomes in TE buffer. The confocal volume (~0.5 fl) was calibrated using a tetramethylrhodamine solution. The excitation power was kept low (~50 μW) to minimize photobleaching and triplet formation.

The cross-correlation function is defined as[20,21,42]

$$G_{1\text{-}2}(\tau) = \frac{\langle \delta I_1(t)\delta I_2(t+\tau)\rangle}{\langle I_1(t)\rangle\langle I_2(t)\rangle} \quad (6)$$

where $I_{1,2}(t)$ represents the fluorescence signal measured in detectors 1 and 2 at time t; angled brackets denote time averages; and $\delta I_{1,2}(t)$, the fluctuations of the fluorescence signal, are defined as the deviations from the temporal average: $\delta I_{1,2}(t) = I_{1,2}(t) - \langle I_{1,2}(t)\rangle$. (This definition is strictly the normalized cross-covariance. The definitions of the autocorrelation function and autocovariance function are frequently used interchangeably in the FCS literature and other applications of fluctuation analysis[42].) In this experiment, detectors 1 and 2 both measure the donor signal, and thus the cross-correlation function defined above is identical to the donor autocorrelation function in the absence of after-pulsing effects.

The autocorrelation function describing the fluctuations in fluorescence intensity of nucleosomes labeled with donor only, that are freely diffusing in three dimensions with a diffusion coefficient D, is given by[20,21]

$$G_D(\tau) = \frac{1}{V_{\text{eff}}\langle C\rangle}\frac{1}{\left(1+\frac{4D\tau}{r_0^2}\right)}\frac{1}{\left(1+\frac{4D\tau}{z_0^2}\right)^{1/2}} \quad (7)$$

where $V_{\text{eff}} = \pi^{3/2} r_0^2 z_0$ represents the effective confocal volume; $\langle C\rangle$ is the mean concentration of particles in the sample; and r_0 and z_0 are the radial and axial dimensions of the observation volume, respectively.

For a nucleosome sample containing both donor and acceptor, the opening and closing of the DNA as the nucleosome diffuses through the confocal volume represent an extra source of fluorescence fluctuations. Assuming a two-state model,

$$\mathrm{N} \underset{k_{21}}{\overset{k_{12}}{\rightleftharpoons}} \mathrm{S} \quad (8)$$

the autocorrelation function is given by[20,21]

where F represents the fraction of dark molecules (fully wrapped nucleosomes). This equation assumes that the dark state is completely dark—in other words,

$$G_{DA}(\tau) = \frac{1}{V_{\text{eff}}\langle C\rangle}\frac{1}{\left(1+\frac{4D\tau}{r_0^2}\right)}\frac{1}{\left(1+\frac{4D\tau}{z_0^2}\right)^{1/2}}\left(1+\frac{F}{1-F}e^{-t(k_{12}+k_{21})}\right) \quad (9)$$

that there is no residual fluorescence. Consistent with our bulk measurements, experiments on single diffusing D-A-labeled nucleosomes showed that the FRET efficiency of the closed form is 0.95 (data not shown), thus, corrections to equation (9) are unnecessary.

The ratio of equations (9) and (7) yields

$$\frac{G_{DA}(\tau)}{G_D(\tau)} = 1 + \frac{F}{1-F}e^{-t(k_{12}+k_{21})} \quad (10)$$

where F, the fraction of dark states, can be expressed as $k_{21} / (k_{21} + k_{12})$. The pre-exponential factor in equation (10) can be rewritten in terms of the equilibrium constant of the closed to open reaction as

$$F(1-F) = k_{21} / k_{12} = 1 / K_{\text{eq}} \quad (11)$$

Note: Supplementary information is available on the Nature Structural & Molecular Biology website.

ACKNOWLEDGMENTS

We are grateful to S. Huang for valuable discussions and comments on the manuscript. We thank J. Little for the LexA expression plasmid, and the Keck Biophysics Facility at Northwestern University for the use of instruments. This work was supported by US National Institutes of Health (NIH) grants GM54692 and GM58617 to J.W., and by NIH grant GM32543, and US Department of Energy grants DE-AC03-76DF00098, GTL2BN Microscopies of Molecular Machines, and SNANOB Design of Autonomous Nanobots to C.B.

COMPETING INTERESTS STATEMENT

The authors declare that they have no competing financial interests.

Received 9 September; accepted 4 November 2004

Published online at http://www.nature.com/nsmb/

1. Richmond, T. & Widom, J. Nucleosome and chromatin structure. In *Chromatin Structure and Gene Expression* (eds. Eligin, S.C.R. & Workman, J.L.) (Oxford Univ. Press, Oxford, 2000).
2. Richmond, T.J. & Davey, C.A. The structure of DNA in the nucleosome core. *Nature* **423**, 145–150 (2003).
3. Kornberg, R.D. & Lorch, Y. Twenty-five years of the nucleosome, fundamental particle of the eukaryote chromosome. *Cell* **98**, 285–294 (1999).
4. Felsenfeld, G. & Groudine, M. Controlling the double helix. *Nature* **421**, 448–453 (2003).
5. Felsenfeld, G. Chromatin unfolds. *Cell* **86**, 13–19 (1996).
6. Khorasanizadeh, S. The nucleosome: from genomic organization to genomic regulation. *Cell* **116**, 259–272 (2004).
7. Langst, G. & Becker, P.B. Nucleosome remodeling: one mechanism, many phenomena? *Biochim. Biophys. Acta* **1677**, 58–63 (2004).
8. Muchardt, C. & Yaniv, M. ATP-dependent chromatin remodelling: SWI/SNF and Co. are on the job. *J. Mol. Biol.* **293**, 187–198 (1999).
9. Narlikar, G.J., Fan, H.Y. & Kingston, R.E. Cooperation between complexes that regulate chromatin structure and transcription. *Cell* **108**, 475–487 (2002).
10. Peterson, C.L. & Logie, C. Recruitment of chromatin remodeling machines. *J. Cell. Biochem.* **78**, 179–185 (2000).
11. Polach, K.J. & Widom, J. Mechanism of protein access to specific DNA sequences in chromatin: a dynamic equilibrium model for gene regulation. *J. Mol. Biol.* **254**, 130–149 (1995).
12. Anderson, J.D. & Widom, J. Sequence and position-dependence of the equilibrium accessibility of nucleosomal DNA target sites. *J. Mol. Biol.* **296**, 979–987 (2000).
13. Clegg, R.M. Fluorescence resonance energy transfer and nucleic acids. *Methods Enzymol.* **211**, 353–388 (1992).
14. Li, G. & Widom, J. Nucleosomes facilitate their own invasion. *Nat. Struct. Mol. Biol.* **11**, 763–769 (2004).
15. Feynman, R.P., Leighton, R.B. & Sands, M. *The Feynman Lectures on Physics* (Addison-Wesley, Reading, Massachusetts, USA, 1963).
16. Fan, H.Y., He, X., Kingston, R.E. & Narlikar, G.J. Distinct strategies to make nucleosomal DNA accessible. *Mol. Cell* **11**, 1311–1322 (2003).
17. Kassabov, S.R., Zhang, B., Persinger, J. & Bartholomew, B. SWI/SNF unwraps, slides, and rewraps the nucleosome. *Mol. Cell* **11**, 391–403 (2003).
18. Protacio, R.U., Polach, K.J. & Widom, J. Coupled-enzymatic assays for the rate and mechanism of DNA site exposure in a nucleosome. *J. Mol. Biol.* **274**, 708–721 (1997).
19. Bonnet, G., Krichevsky, O. & Libchaber, A. Kinetics of conformational fluctuations in DNA hairpin-loops. *Proc. Natl. Acad. Sci. USA* **95**, 8602–8606 (1998).
20. Hess, S.T., Huang, S., Heikal, A.A. & Webb, W.W. Biological and chemical applications of fluorescence correlation spectroscopy: a review. *Biochemistry* **41**, 697–705 (2002).
21. Krichevsky, O. & Bonnet, G. Fluorescence correlation spectroscopy: the technique and its applications. *Rep. Prog. Phys.* **65**, 251–297 (2002).
22. Ha, T. *et al.* Initiation and re-initiation of DNA unwinding by the *Escherichia coli* Rep helicase. *Nature* **419**, 638–641 (2002).
23. Halford, S.E. & Marko, J.F. How do site-specific DNA-binding proteins find their targets? *Nucleic Acids Res.* **32**, 3040–3052 (2004).

24. von Hippel, P.H. & Berg, O.G. Facilitated target location in biological systems. *J. Biol. Chem.* **264**, 675–678 (1989).
25. Owen-Hughes, T. & Workman, J.L. Remodeling the chromatin structure of a nucleosome array by transcription factor-targeted trans-displacement of histones. *EMBO J.* **15**, 4702–4712 (1996).
26. Owen-Hughes, T., Utley, R.T., Cote, J., Peterson, C.L. & Workman, J.L. Persistent site-specific remodeling of a nucleosome array by transient action of the SWI/SNF complex. *Science* **273**, 513–516 (1996).
27. Logie, C. & Peterson, C.L. Catalytic activity of the yeast SWI/SNF complex on reconstituted nucleosome arrays. *EMBO J.* **16**, 6772–6782 (1997).
28. Beard, D.A. & Schlick, T. Computational modeling predicts the structure and dynamics of chromatin fiber. *Structure* **9**, 105–114 (2001).
29. Widom, J. Structure, dynamics, and function of chromatin in vitro. *Annu. Rev. Biophys. Biomol. Struct.* **27**, 285–327 (1998).
30. Widom, J. Chromatin structure: linking structure to function with histone H1. *Curr. Biol.* **8**, R788–R791 (1998).
31. Widom, J. Toward a unified model of chromatin folding. *Annu. Rev. Biophys. Biophys. Chem.* **18**, 365–395 (1989).
32. Escher, D. & Schaffner, W. Gene activation at a distance and telomeric silencing are not affected by yeast histone H1. *Mol. Gen. Genet.* **256**, 456–461 (1997).
33. Patterton, H.G., Landel, C.C., Landsman, D., Peterson, C.L. & Simpson, R.T. The biochemical and phenotypic characterization of Hho1p, the putative linker histone H1 of Saccharomyces cerevisiae. *J. Biol. Chem.* **273**, 7268–7276 (1998).
34. Freidkin, I. & Katcoff, D.J. Specific distribution of the *Saccharomyces cerevisiae* linker histone homolog HHO1p in the chromatin. *Nucleic Acids Res.* **29**, 4043–4051 (2001).
35. Cloutier, T.E. & Widom, J. Spontaneous sharp bending of double-stranded DNA. *Mol. Cell* **14**, 355–362 (2004).
36. Narlikar, G.J., Phelan, M.L. & Kingston, R.E. Generation and interconversion of multiple distinct nucleosomal states as a mechanism for catalyzing chromatin fluidity. *Mol. Cell* **8**, 1219–1230 (2001).
37. Shermoen, A.W. & O'Farrell, P.H. Progression of the cell cycle through mitosis leads to abortion of nascent transcripts. *Cell* **67**, 303–310 (1991).
38. Thastrom, A., Bingham, L.M. & Widom, J. Nucleosomal locations of dominant DNA sequence motifs for histone-DNA interactions and nucleosome positioning. *J. Mol. Biol.* **338**, 695–709 (2004).
39. Little, J.W. *et al.* Cleavage of LexA repressor. *Methods Enzymol.* **244**, 266–284 (1994).
40. Kim, B. & Little, J.W. Dimerization of a specific DNA-binding protein on the DNA. *Science* **255**, 203–206 (1992).
41. Bernasconi, C.F. (ed.). Investigation of rates and mechanisms of reactions. In *Techniques of Chemistry* 4th edn. Vol. VI (Wiley, New York, 1986).
42. Widengren, J. & Mets, U. Conceptual basis of fluorescence correlation spectroscopy and related techniques as tools in bioscience. In *Single Molecule Detection in Solution* (eds. Zander, C., Enderlein, J. & Keller, R.A.) 69–120 (Wiley-VCH, Berlin, 2002).